Letter

Critical-like slowdown in thermal soft-sphere glasses via energy minimization

Kevin A. Interiano-Alberto,[1] Peter K. Morse,[2] and Robert S. Hoy[1,*]
[1]*Department of Physics, University of South Florida, Tampa, Florida 33620, USA*
[2]*Department of Chemistry, Department of Physics, and Princeton Institute of Materials, Princeton University, Princeton, New Jersey 08544, USA*

(Received 20 December 2023; revised 15 April 2024; accepted 3 June 2024; published 24 June 2024)

Using hybrid molecular dynamics/SWAP Monte Carlo (MD/SMC) simulations, we show that while the terminal relaxation times $\tau(\phi)$ for FIRE energy minimization of soft-sphere glasses can decrease by orders of magnitude as sample equilibration proceeds and the jamming density ϕ_J increases, they always scale as $\tau(\phi) \sim (\phi_J - \phi)^{-2} \sim [Z_{iso} - Z_{ms}(\tau)]^{-2}$, where $Z_{iso} = 2d$ and $Z_{ms}(\tau)$ is the average coordination number of particles satisfying a minimal local mechanical stability criterion ($Z \geqslant d + 1$) *at the top of* the final potential-energy-landscape (PEL) sub-basin the system encounters. This scaling allows us to collapse τ datasets that look very different when plotted as a function of ϕ, and to address a closely related question: how does the character of the PEL basins that dense thermal glasses *most typically* occupy evolve as the glasses age at constant ϕ and T?

DOI: 10.1103/PhysRevE.109.L062603

Jamming exhibits many features that are reminiscent of critical phenomena [1]. Since multiple length and time scales exhibit power-law divergences as ϕ_J is approached from below [2–5], so do their associated mechanical quantities. For example, the shear viscosity of colloidal suspensions (η), which is often assumed to be linearly proportional to their characteristic stress-relaxation time τ_{visc}, scales as $\eta \sim |\Delta\phi|^{-\beta}$, where $\Delta\phi = \phi - \phi_J$ is the excess packing fraction, and $1.6 \leqslant \beta \leqslant 4$ [6–13]. Correspondingly, recent simulations have shown that the characteristic relaxation times (τ^*) for energy minimization and shear-stress relaxation in *athermal* hard and soft sphere glasses scale as $\tau^* \sim |\Delta Z|^{-\nu}$, where $\Delta Z = Z - Z_{iso} \equiv Z - 2d$ is the excess coordination number, and $1.6 \lesssim \nu \lesssim 3.7$ [14–21]. These divergences can be understood in terms of the relation $\tau^* \sim \omega_{min}^{-2}$, where ω_{min} is the frequency of systems' lowest-energy vibrational mode [16,17]. Such modes increasingly dominate systems' relaxation dynamics as $\phi \to \phi_J$ from below and $\omega_{min} \to 0$ [16–20,22]. Assuming that they control η for densities just below jamming, and employing the relation $\Delta Z \sim \Delta\phi$, allows the abovementioned scaling relation to be re-expressed as $\eta \sim \tau^* \sim |\Delta Z|^{-\nu}$, if in fact $\beta = \nu$ as suggested by Refs. [14–20].

A recent study [21] has challenged some of the main conclusions of Refs. [16–20], and in particular their assertions that (i) the divergence of τ^* represents a true critical phenomenon with a well-defined value of ν, and (ii) athermal glasses' τ_{visc} and η are both controlled by τ^*. On the other hand, the critical-*like* slowdown of *athermal* soft-sphere glasses' energy-minimization and shear-stress-relaxation dynamics as $\phi \to \phi_J$ and $Z \to Z_{iso}$ from below is now well established. The extent to which these phenomena affect *thermal* glasses' relaxation dynamics, and hence are subject to "onset" effects, however, has not been explored. Thermalized 3D hard-sphere liquids equilibrated at packing fractions ϕ_{eq} below the onset density $\phi_{on} \simeq 0.45$ always have the same jamming density $\phi_J = \phi_{RCP} \simeq 0.64$ [23], while those equilibrated at $\phi_{eq} > \phi_{on}$ have ϕ_J that increase with increasing ϕ_{eq}, or, for fixed ϕ_{eq}, with increasing equilibration time t_{eq} [23–26]. Similarly, soft-sphere liquids equilibrated at fixed ϕ and temperatures T above the onset temperature $T_{on}(\phi)$ always have the same average inherent structure energy (E_{IS}), while those equilibrated at temperatures $T < T_{on}$ have E_{IS} that decrease with decreasing T and increasing t_{eq} [27,28]. Because Refs. [6–21] all examined systems where $\phi_J \simeq \phi_{RCP}$, a natural followup question is: how are the divergences of time scales like τ^* affected by sample preparation/thermal onset, i.e., by the abovementioned increasing $\phi_J(t_{eq})$ and decreasing $T_{on}(\phi, t_{eq})$?

In this Letter, using MD/SMC simulations combined with FIRE energy minimization [29–32], we shed light on this question. By starting with far-from-equilibrium soft-sphere glasses obtained via infinite-temperature quenches (with a wide range of ϕ) and then bringing them toward equilibrium using SWAP, we show that the times τ required for thermal soft-sphere glasses to enter their final unjammed potential-energy-landscape (PEL) sub-basin during energy minimization exhibit thermal onset as samples become increasingly well equilibrated, in the same fashion that $\phi_J(t_{eq})$ does. Although $\tau(\phi, t_{eq})$ can decrease by orders of magnitude as equilibration proceeds and $\phi_J(t_{eq})$ increases via thermal onset, it always scales as $\tau(\phi, t_{eq}) \sim [\phi_J(t_{eq}) - \phi]^{-2} \sim \Delta Z^{-2}$, where $\Delta Z \equiv Z_{iso} - Z_{ms}[\tau(\phi, t_{eq})]$, for sufficiently small $\Delta\phi$ and ΔZ. This common scaling allows us to collapse τ datasets that look very different when plotted as a function of ϕ and t_{eq}, and thus to greatly simplify our understanding of dense thermal soft-sphere glasses' strongly ϕ- and t_{eq}-dependent energy-minimization dynamics by showing that they are

*Contact author: rshoy@usf.edu

always controlled by the lowest-lying structure of systems' PELs.

All simulations were performed using hdMD [33]. Systems are initialized by placing $N = 10^5$ soft-sphere particles randomly within periodic 3D cubic simulation cells, with a wide range of packing fractions ($0.63 \leqslant \phi \leqslant 0.68$). These particles are continuously polydisperse, with a size distribution that produces excellent glass-formability for a variety of pair potentials [30,34,37]. Infinite-temperature quenches are performed [1], and then systems are equilibrated at a constant temperature $k_B T_{\rm eq} = \tilde{\epsilon}$ using the SWAP algorithm [29,30], for times $t_{\rm eq}$ up to $10^5\tilde{\tau}$. Our implementation attempts $N/10$ particle-diameter swaps per $\tilde{\tau}$. Here $\tilde{\tau} = \sqrt{\tilde{m}\tilde{\sigma}^2/\tilde{\epsilon}}$ is the unit of time and $\tilde{m}$, $\tilde{\sigma}$, and $\tilde{\epsilon}$ are, respectively, the units of mass, length, and energy; below, we will express all quantities in terms of these units. For most ϕ examined here, this procedure produces weakly-to-moderately aged glasses (i.e., *not* equilibrated supercooled liquids), consistent with our goal of studying nonequlibrium phenomena that occur deep in the glassy state.

At selected values of $t_{\rm eq}$, we minimize systems' energies using the FIRE [31,32] algorithm. During these minimizations, we monitor changes in the average pair energy per particle $E_{\rm p} = N^{-1}\sum_{j>i} U(r_{ij})$ as well as Z and $Z_{\rm ms}$, which are, respectively, the average coordination numbers for all particles and for all particles i that satisfy a *minimal, local* mechanical stability criterion $Z_i \equiv \sum_{j\neq i}\Theta(\sigma_{ij} - r_{ij}) \geqslant d + 1$ [38,39]. Here r_{ij} is the distance between particles i and j, σ_{ij} is their reduced interparticle diameter [34], Θ is the Heaviside step function, and interparticle contacts are identified using the standard criterion $r_{ij} < \sigma_{ij}$ [1]. Below, we plot these quantities as a function of the elapsed minimization time

$$t = \sum_{i=0}^{I} \delta t_i \tag{1}$$

after I FIRE iterations, where δt_i is the adaptive timestep during the ith iteration [32]. Energy minimization continues until $E_{\rm p}$ reaches zero, $E_{\rm p}$ has not changed over the past ten iterations, or I reaches 10^5 [34]. Since FIRE dynamics are only partially physical (in contrast to steepest-descent dynamics, which correspond to the limit of infinite damping [34,40,41]), we will not assign any physical significance to absolute values of t; below, we will only make relative statements.

We begin by discussing the ϕ and t dependence of E_p, Z, and Z_{ms} for one representative $t_{\rm eq}$ value (6×10^4). Figure 1(a) shows $E_{\rm p}(t)$ data for systems with $.655 \leqslant \phi \leqslant .675$, in increments $\delta\phi = .0005$. During the initial stages of energy minimization, all systems have $E_{\rm p}(t) \sim t^{-1}$ [19]. In jammed systems, $\partial E_{\rm p}/\partial t$ increases monotonically with t, and $E_{\rm p}$ converges faster as ϕ increases, consistent with previous studies [42–45]. For unjammed systems, the response is qualitatively different. The initial $E_{\rm p}(t) \sim t^{-1}$ regimes end at times $t_{\rm drop}(\phi)$. Over a wide range of ϕ and $t > t_{\rm drop}(\phi)$, $E_{\rm p}(t) \sim \exp[-t/\tau^*(\phi)]$, where (consistent with previous studies [16–20]) $\tau^* \sim (\phi_{\rm J} - \phi)^{-2}$ as $\phi \to \phi_{\rm J}$ from below [34]. However, $E_{\rm p}$ does not smoothly drop all the way to zero as might be expected. Instead, the exponentially decaying portions of the $E_{\rm p}(t)$ curves end at finite $E_{\rm p}$, exhibiting kinks at times $\tau(\phi)$ that increase rapidly with ϕ. During the final stages of minimization, $E_{\rm p}$ drops toward zero in a roughly power-law fashion. Overall, the $E_{\rm p}(t)$ dataset suggests that the kinks for $\phi < \phi_{\rm J}$ correspond to systems entering their final PEL sub-basin.

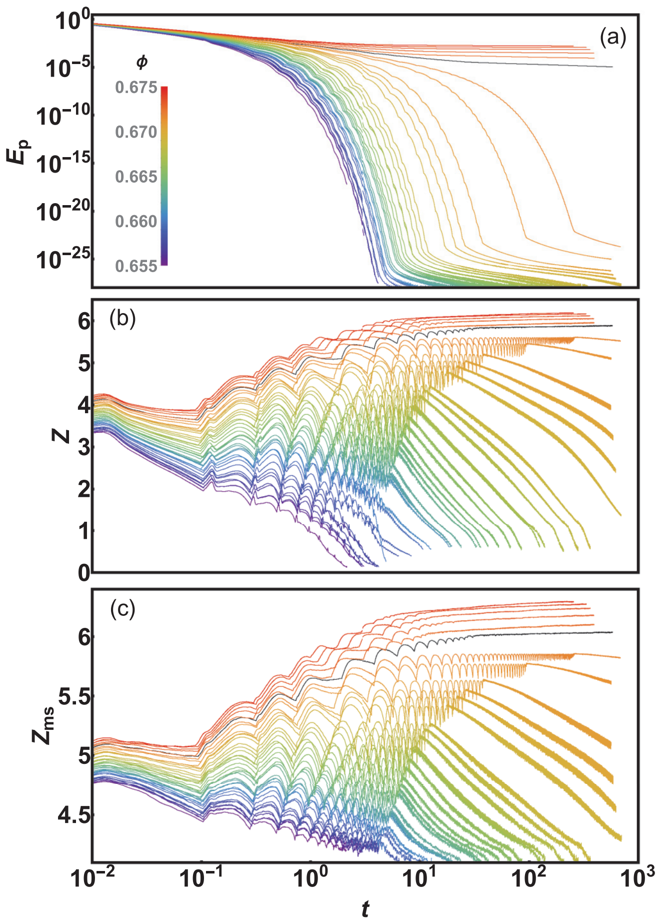

FIG. 1. Structural metrics during FIRE energy minimization of 3D thermal soft-sphere glasses equilibrated for $t_{\rm eq} = 6 \times 10^4$. This system has $\phi_{\rm J}(t_{\rm eq}) = 0.6726$ [from Eq. (2)]; black curves indicate results for the lowest $\phi \gtrsim \phi_{\rm J}$.

This hypothesis is strongly supported by examining the coordination number $Z(t)$. As shown in Fig. 1(b), the $Z(t)$ exhibit a common behavior for small t, first decreasing and then increasing as the elimination of strong interparticle overlaps brings more particles into contact with each other. For $\phi \geqslant \phi_{\rm J}$, these increases persist to $t \to \infty$ as is typical of jammed systems [1]. For $\phi < \phi_{\rm J}$, however, they terminate at the same finite $\tau(\phi)$ shown in panel (a). For $t > \tau(\phi)$, the $Z(t)$ [much like the $E_{\rm p}(t)$] drop slowly toward zero. At intermediate times, $Z(t)$ oscillates. The local minima in $Z(t)$ coincide with the FIRE algorithm resetting when the system encounters a saddle point and the dot product of the N-particle force and velocity vectors ($\vec{F} \cdot \vec{v}$) for a *prospective* set of particle positions $\{r\}$ becomes negative [31]. After these resetting events, Z tends to first increase as a few larger interparticle overlaps get converted into many smaller ones, then decrease again as these small overlaps are eliminated. Since this occurs when the system traverses a region in which the direction of $\vec{F}$ is changing substantially from one iteration to the next, the oscillations cease once it has entered its final PEL sub-basin [at $t = \tau(\phi)$]. Figure 1(c) shows that the character of these oscillations is not changed by removing particles with $Z_i < d + 1$ [34,38]. Note, however, that for both $Z(t)$ and $Z_{\rm ms}(t)$ their amplitude decreases and their frequency increases as $\phi \to \phi_{\rm J}$.

We find that τ is always linearly proportional to (albeit substantially larger than [34]) τ^*, indicating that the results reported above are closely related to those discussed in Refs. [16–20]. Since these studies employed either normal MD time integration (in simulations of shear stress relaxation) or gradient-descent rather than FIRE energy minimization, they were unable to observe the kinks in $E_{\rm p}(t)$ and oscillations in $Z(t)$ and $Z_{\rm ms}(t)$ discussed above, or to measure an exact analog to the terminal relaxation time τ. As we will demonstrate below, the utility of the above discussion is that it allows us to convincingly argue that $\Delta Z(\tau) \equiv Z_{\rm iso} - Z_{\rm ms}(\tau)$, i.e., minimally-locally-stable particles' average hypostaticity at the top of the final sub-basin the system encounters, is a well-defined quantity that can be used to describe these systems' energy-minimization dynamics.

Our main contribution centers around the fact that the only substantial changes in the phenomona illustrated in Fig. 1 as $t_{\rm eq}$ increases are that they shift to higher ϕ, following the increase in $\phi_{\rm J}(t_{\rm eq})$ as thermal onset proceeds. We observe exponential decay of E_p terminating in kinks at $t = \tau(\phi, t_{\rm eq})$, oscillations in Z and $Z_{\rm ms}$, and divergences in $\tau \sim \tau^*$ as $\phi \to \phi_{\rm J}(t_{\rm eq})$ from below, for all values of $t_{\rm eq}$ [34]. Results for $\tau(\phi, t_{\rm eq})$ for a wide range of ϕ and $t_{\rm eq}$ are summarized in Fig. 2. Panel (a) shows how the jamming densities $\phi_{\rm J}(t_{eq})$ obtained by fitting the finite $[\phi < \phi_{\rm J}(t_{\rm eq})]$ τ values to the empirical formula

$$\tau(\phi, t_{\rm eq}) = A(t_{\rm eq}) + \frac{B(t_{\rm eq})}{[\phi_{\rm J}(t_{\rm eq}) - \phi]^2} \quad (2)$$

increase via thermal onset; $\phi_{\rm J}(t_{\rm eq})$ increases roughly logarithmically with $t_{\rm eq}$, from $\sim$0.648 to $\sim$0.674 over the range $10^1 \leqslant t_{\rm eq} \leqslant 10^5$. Comparable increases in $\phi_{\rm J}(t_{\rm eq})$ have been reported before—they arise from relatively well understood thermal onset effects [24–28]—but the concomitant shift of the ranges of $\phi < \phi_{\rm J}(t_{\rm eq})$ over which relaxation times for energy minimization diverge has been reported on very little (if at all).

Panel (b) illustrates a closely associated effect. When $\phi_{\rm J}(t_{\rm eq}) < \phi$, τ values are effectively infinite since systems never unjam. As thermal onset proceeds, τ values become finite (but large) as soon as $\phi_{\rm J}(t_{\rm eq})$ exceeds ϕ, then drop by $\sim$2 orders of magnitude as systems approach equilibrium. Below, we will interpret this result in terms of how thermal soft-sphere glasses' most-typically-occupied PEL basins evolve during constant-ϕ aging, and suggest how it might be experimentally characterized.

Panel (c) shows that τ diverges with increasing $Z_{\rm ms}(\tau)$ approximately as

$$\tau(\phi, t_{\rm eq}) = C + \frac{D}{(Z_{\rm iso} - Z_{\rm ms}[\tau(\phi, t_{\rm eq})])^2}, \quad (3)$$

where C and D are $t_{\rm eq}$-independent constants. The common inverse-quadratic form of the diverging time scales illustrated in panels (a) and (c) arises rather trivially since $Z_{\rm ms}(\tau)$

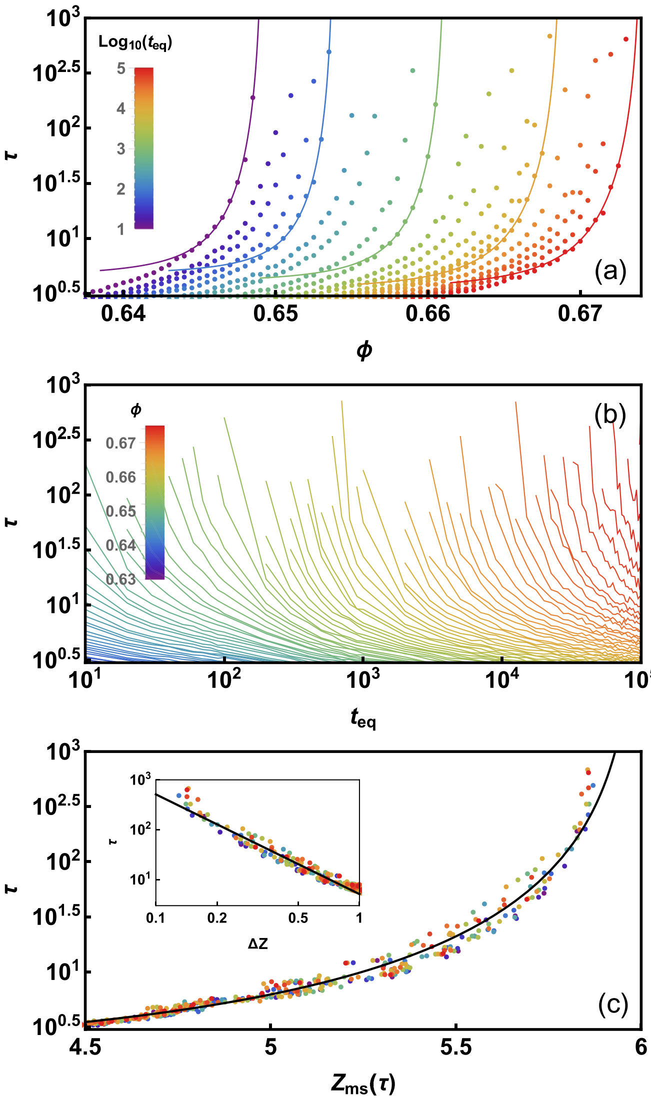

FIG. 2. Effect of thermal onset on soft-sphere glasses' energy-minimization dynamics. Panels (a) and (c), respectively, show τ vs ϕ and $Z_{\rm ms}(\tau)$ for selected $t_{\rm eq}$, while panel (b) shows τ vs $t_{\rm eq}$ for selected ϕ. Solid curves in panel (a) show fits to Eq. (2) for $t_{\rm eq} = 10^1$, 10^2, 10^3, 10^4, and 10^5. In panel (c), the color legend is the same as in panel (a), the solid curve shows a single fit of the entire dataset to Eq. (3) with $C = 1.55$ and $D = 4.86$, and the inset shows the same data plotted vs ΔZ, with a line indicating ΔZ^{-2} scaling.

increases linearly with ϕ over the range of packing fractions for which Eqs. (2) and (3) describe the data.

We emphasize that [owing to the concerns raised in Ref. [21] and the upturns in τ at small ΔZ that are visible in Fig. 2(c)] we are *not* asserting that the above results imply a true critical phenomenon with $\nu = 2$. Employing a different energy-minimization algorithm can change the values of both τ and ν [34,40,41], and our goal for this study is not to formulate an exact physics picture for $\tau(\phi, t_{\rm eq})$. On the other hand, the results presented in panel (c) [unlike those of panel (a)] unambiguously show that (i) plotting the terminal relaxation times for thermal glasses' energy minimization as a function of the $Z_{\rm ms}$ values at those times allows one to collapse results that look very different when plotted as a function of ϕ, and

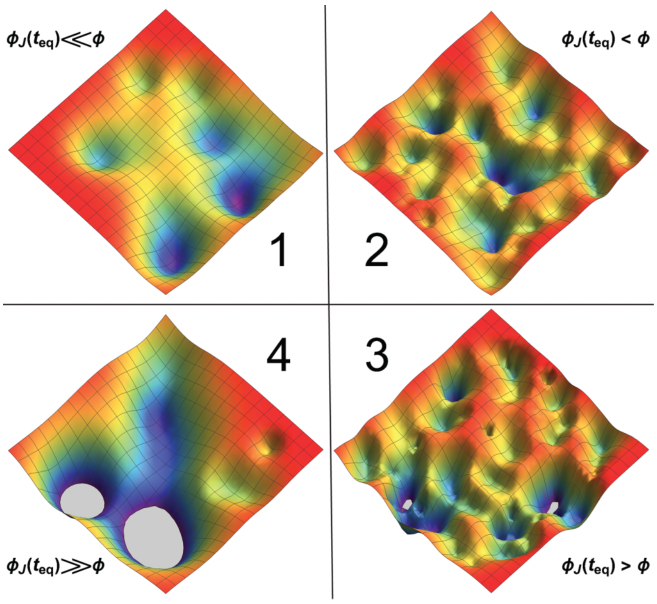

FIG. 3. Schematic illustration of how the PEL regions most typically sampled by thermal soft-sphere glasses evolve as they age at constant ϕ and T following a thermal quench. Unjammed regions of the PEL are gray-colored.

(ii) these times always diverge when systems are isostatic at the top of the final PEL sub-basin they encounter.

Results (i) and (ii) allow us to formulate a simplified picture of these systems' strongly ϕ- and t_{eq}-dependent energy-minimization dynamics. The data shown in Fig. 2(a) would paint a very confusing picture if the color coding were removed, or if one attempted to compare results for systems that had been prepared using different equilibration protocols. In contrast, Fig. 2(c) is much easier to understand. It shows that the terminal relaxation times for energy minimization in thermalized soft-sphere glasses are always controlled by the lowest-lying structure of systems' PELs. This structure can evolve *dramatically* with equilibration or "waiting" time owing to thermal onset, but the collapse illustrated in Fig. 2(c) shows that the effects of this evolution on $\tau(\phi, t_{eq})$ can be understood almost trivially. This is the central result of our study. Our demonstration that $Z_{ms}[\tau(\phi, t_{eq})]$ rather than ϕ is the relevant control variable for thermal soft-sphere glasses' energy-minimization dynamics might also serve as the basis for a critical-phenomena-based theory for these dynamics, formulated along the lines of Refs. [46,47].

All trends reported above indicate that systems spend a diverging amount of time near the boundaries between sub-basins that have large Z but very small E_p, and that they encounter more and more of these boundaries as $\phi \to \phi_J(t_{eq})$ from below. This is consistent with the Gardner-like-physics prediction of a proliferation of sub-basins with very small but nonzero energy [48,49], and with recent studies suggesting that glasses subjected to thermal quenches spend a diverging amount of time (as $\phi \to \phi_J$ from below) traversing saddle points as they explore their PELs and gradually fall into ever-lower sub-basins before finally unjamming [42–45,50,51]. The proliferation of kinks, since they correspond to changes of direction of $\vec{F}$ and $\vec{v}$, agrees with Ref. [52]'s demonstration that systems near jamming follow fractal paths through configuration space during FIRE energy minimization.

Taken together, our results suggest the following four-stage picture (schematically illustrated in Fig. 3) for how the character of the PEL basins that simulated dense thermal soft-sphere glasses *most typically* occupy evolves as they are equilibrated at constant ϕ and T following a thermal quench: (i) When t_{eq} is small and $\phi_J(t_{eq})$ remains well below ϕ, systems are typically in a smooth portion of their PEL and can quickly find the bottom of a nearby jammed basin; (ii) As $\phi_J(t_{eq})$ approaches ϕ from below, systems cross into rougher portions of their PELs that have more "wrinkles" (basin boundaries), and hence take longer to find the bottom of a jammed basin; (iii) As $\phi_J(t_{eq})$ increases past ϕ, unjammed basins emerge, but to reach them, systems must traverse very rough regions of their PELs characterized by a proliferation of basins with fractal boundaries [49,52]; and (iv) Finally, as $t_{eq} \to \infty$ and $\phi_J(t_{eq})$ grows further beyond ϕ, systems cross back into progressively smoother portions of their PELs where they can more quickly find the bottom of a nearby unjammed basin.

Numerous studies have shown that both athermal and quenched glasses go through this process as ϕ decreases from well above to well below ϕ_{RCP} [20,43,44,49,53,54]. Here we have argued that it should also occur in sufficiently-dense thermal glasses maintained at fixed ϕ and T, as their thermalized pair energy $E_p(t_{eq})$ and pressure $P(t_{eq})$ slowly decrease via aging [55,56]. Since the transition from stage (ii) to stage (iii) is associated with both diverging length scales [2,16,21] and diverging time scales such as τ^*, τ, and ω_{min}^{-1}, it should have multiple signatures whose observation does not require energy minimization. For example, it should also produce a nonmonotonic evolution of systems' low-energy vibrational spectra that should be easily observable in simulations [57,58] and potentially observable in experiments [59–61]. Finally we point out that stage (iv) can be interpreted as an extension of the well-known reduction of $E_{IS}(\phi)$ with increasing t_{eq} [27,28]. While $E_{IS}(\phi, t_{eq}) = 0$ for all systems that ultimately unjam, i.e.. for all $t_{eq} > t_{unjam}(\phi)$, thermal onset continues even for $t_{eq} > t_{unjam}(\phi)$, in the sense that systems continue moving into progressively-smoother regions of their PELs where the unjammed basins are both larger and more easily accessible.

We thank P. Charbonneau for helpful discussions. This material is based upon work supported by the National Science Foundation under Grants No. DMR-2026271 and No. DMR-2419261.

[1] C. S. O'Hern, L. E. Silbert, A. J. Liu, and S. R. Nagel, Jamming at zero temperature and zero applied stress: The epitome of disorder, Phys. Rev. E **68**, 011306 (2003).

[2] M. Wyart, S. R. Nagel, and T. A. Witten, Geometric origin of excess low-frequency vibrational modes in weakly connected amorphous solids, Europhys. Lett. **72**, 486 (2005).

[3] A. S. Keys, A. R. Abate, S. C. Glotzer, and D. J. Durian, Measurement of growing dynamical length scales and prediction of the jamming transition in a granular material, Nat. Phys. **3**, 260 (2007).

[4] A. B. Hopkins, F. H. Stillinger, and S. Torquato, Nonequilibrium static diverging lengthscales on approaching a prototypical model glassy state, Phys. Rev. E **86**, 021505 (2012).

[5] L. Berthier, P. Charbonneau, Y. Jin, G. Parisi, B. Seoane, and F. Zamponi, Growing timescales and lengthscales characterizing vibrations of amorphous solids, Proc. Natl. Acad. Sci. USA **113**, 8397 (2016).

[6] J. F. Brady, The rheological behavior of concentrated colloidal dispersions, J. Chem. Phys. **99**, 567 (1993).

[7] P. Olsson and S. Teitel, Critical scaling of shear viscosity at the jamming transition, Phys. Rev. Lett. **99**, 178001 (2007).

[8] Y. Forterre and O. Pouliquen, Flows of dense granular media, Annu. Rev. Fluid Mech. **40**, 1 (2008).

[9] K. N. Nordstrom, E. Verneuil, P. E. Arratia, A. Basu, Z. Zhang, A. G. Yodh, J. P. Gollub, and D. J. Durian, Microfluidic rheology of soft colloids above and below jamming, Phys. Rev. Lett. **105**, 175701 (2010).

[10] F. Boyer, E. Guazzelli, and O. Pouliquen, Unifying suspension and granular rheology, Phys. Rev. Lett. **107**, 188301 (2011).

[11] B. Andreotti, J.-L. Barrat, and C. Heussinger, Shear flow of non-Brownian suspensions close to jamming, Phys. Rev. Lett. **109**, 105901 (2012).

[12] T. Kawasaki, D. Coslovich, A. Ikeda, and L. Berthier, Diverging viscosity and soft granular rheology in non-Brownian suspensions, Phys. Rev. E **91**, 012203 (2015).

[13] K. Suzuki and H. Hayakawa, Divergence of viscosity in jammed granular materials: A theoretical approach, Phys. Rev. Lett. **115**, 098001 (2015).

[14] C. Heussinger and J.-L. Barrat, Jamming transition as probed by quasistatic shear flow, Phys. Rev. Lett. **102**, 218303 (2009).

[15] P. Olsson, Dimensionality and viscosity exponent in shear-driven jamming, Phys. Rev. Lett. **122**, 108003 (2019).

[16] E. Lerner, G. Düring, and M. Wyart, A unified framework for non-Brownian suspension flows and soft amorphous solids, Proc. Natl. Acad. Sci. USA **109**, 4798 (2012).

[17] E. Lerner, G. Düring, and M. Wyart, Toward a microscopic description of flow near the jamming threshold, Europhys. Lett. **99**, 58003 (2012).

[18] P. Olsson, Relaxation times and rheology in dense athermal suspensions, Phys. Rev. E **91**, 062209 (2015).

[19] A. Ikeda, T. Kawasaki, L. Berthier, K. Saitoh, and T. Hatano, Universal relaxation dynamics of sphere packings below jamming, Phys. Rev. Lett. **124**, 058001 (2020).

[20] K. Saitoh, T. Hatano, A. Ikeda, and B. P. Tighe, Stress relaxation above and below the jamming transition, Phys. Rev. Lett. **124**, 118001 (2020).

[21] Y. Nishikawa, A. Ikeda, and L. Berthier, Relaxation dynamics of non-Brownian spheres below jamming, J. Stat. Phys. **182**, 37 (2021).

[22] Below jamming, one has to use momentum transfer to model the density of states $D(\omega)$. This is usually done using either an effective potential or a Fourier transform of the velocity autocorrelation function.

[23] S. Torquato, T. M. Truskett, and P. G. Debenedetti, Is random close packing of spheres well defined? Phys. Rev. Lett. **84**, 2064 (2000).

[24] P. Chaudhuri, L. Berthier, and S. Sastry, Jamming transitions in amorphous packings of frictionless spheres occur over a continuous range of volume fractions, Phys. Rev. Lett. **104**, 165701 (2010).

[25] M. Ozawa, L. Berthier, and D. Coslovich, Exploring the jamming transition over a wide range of critical densities, SciPost Phys. **3**, 027 (2017).

[26] P. Charbonneau and P. K. Morse, Memory formation in jammed hard spheres, Phys. Rev. Lett. **126**, 088001 (2021).

[27] S. Sastry, P. G. Debenedetti, S. Torquato, and F. H. Stillinger, Signatures of distinct dynamical regimes in the energy landscape of a glass-forming liquid, Nature (London) **393**, 554 (1998).

[28] P. G. Debenedetti and F. H. Stillinger, Supercooled liquids and the glass transition, Nature (London) **410**, 259 (2001).

[29] T. S. Grigera and G. Parisi, Fast Monte Carlo algorithm for supercooled soft spheres, Phys. Rev. E **63**, 045102(R) (2001).

[30] A. Ninarello, L. Berthier, and D. Coslovich, Models and algorithms for the next generation of glass transition studies, Phys. Rev. X **7**, 021039 (2017).

[31] E. Bitzek, P. Koskinen, F. Gähler, M. Moseler, and P. Gumbsch, Structural relaxation made simple, Phys. Rev. Lett. **97**, 170201 (2006).

[32] J. Guénolé, W. G. Nöhring, A. Vaid, F. Houllé, Z. Xie, A. Prakash, and E. Bitzek, Assessment and optimization of the fast inertial relaxation engine (FIRE) for energy minimization in atomistic simulations and its implementation in LAMMPS, Comput. Mater. Sci. **175**, 109584 (2020).

[33] R. S. Hoy and K. A. Interiano-Alberto, Efficient d-dimensional molecular dynamics simulations for studies of the glass-jamming transition, Phys. Rev. E **105**, 055305 (2022).

[34] See Supplemental Material at http://link.aps.org/supplemental/10.1103/PhysRevE.109.L062603, which includes Refs. [35,36], for further details on our (i) interparticle interactions; (ii) implementation of the SWAP and FIRE algorithms; (iii) results for the $t_{\rm eq}$-dependence of $E_{\rm p}(t)$, $Z_{\rm ms}(t)$, $\phi_{\rm J}$, A, and B; (iv) demonstration of the relation of τ to τ^*; and (v) a comparison to results obtained from steepest-descent minimization.

[35] T. Shen, C. Schreck, B. Chakraborty, D. E. Freed, and C. S. O'Hern, Structural relaxation in dense liquids composed of anisotropic particles, Phys. Rev. E **86**, 041303 (2012).

[36] M. Schmiedeberg, T. K. Haxton, S. R. Nagel, and A. J. Liu, Mapping the glassy dynamics of soft spheres onto hard-sphere behavior, Europhys. Lett. **96**, 36010 (2011).

[37] To suppress any fractionation, we employ a polydispersity index ($\Delta = 0.107$) that is lower than that employed in several recent studies. For example, Refs. [25,30] used the same $P(\sigma) \sim \sigma^{-3}$ [34], but with $\Delta = 0.23$.

[38] The $Z_i \geqslant d + 1$ criterion was used to identify non-rattlers in Refs. [15–21], but in contrast to these studies, we do *not* iteratively remove particles with $d + 1$ contacts prior to calculating the final Z values.

[39] P. K. Morse and E. I. Corwin, Local stability of spheres via the convex hull and the radical Voronoi diagram, Phys. Rev. E **108**, 064901 (2023).

[40] The larger ν reported in Refs. [15–21] may arise from the different minimization algorithm they employed (i.e. SD energy minimization produces overdamped dynamics whereas FIRE produces damped inertial dynamics), and/or from their different definition of $Z_{\rm ms}$ [21]. In general, $\tau^* = \omega_{\rm min}^{-2}/2$ is expected only

for *overdamped* minimization dynamics; inertial dynamics give $\tau^* \sim \omega_{\rm min}^{-1}$.

[41] Our τ values are one or more orders of magnitude smaller that the corresponding times for SD minimization for the same systems, and indeed smaller than the τ^* values reported in Refs. [15–21] for systems at comparable $\Delta\phi$, owing to FIRE's more efficient implementation.

[42] P. Olsson, Relaxation times, rheology, and finite size effects for non-Brownian disks in two dimensions, Phys. Rev. E **105**, 034902 (2022).

[43] Y. Nishikawa, M. Ozawa, A. Ikeda, P. Chaudhuri, and L. Berthier, Relazation dynamics in the energy landscape of glass-forming liquids, Phys. Rev. X **12**, 021001 (2022).

[44] A. Manacorda and F. Zamponi, Gradient descent dynamics and the jamming transition in infinite dimensions, J. Phys. A: Math. Theor. **55**, 334001 (2022).

[45] P. Charbonneau and P. K. Morse, Jamming, relaxation, and memory in a minimally structured glass former, Phys. Rev. E **108**, 054102 (2023).

[46] C. P. Goodrich, A. J. Liu, and J. P. Sethna, Scaling ansatz for the jamming transition, Proc. Natl. Acad. Sci. USA **113**, 9745 (2016).

[47] D. B. Liarte, S. J. Thornton, E. Schwen, I. Cohen, D. Chowdhury, and J. P. Sethna, Universal scaling for disordered viscoelastic matter near the onset of rigidity, Phys. Rev. E **106**, L052601 (2022).

[48] E. Gardner, Spin glasses with *p*-spin interactions, Nucl. Phys. B **257**, 747 (1985).

[49] P. Charbonneau, J. Kurchan, G. Parisi, P. Urbani, and F. Zamponi, Fractal free energy landscapes in structural glasses, Nat. Commun. **5**, 3725 (2014).

[50] C. Scalliet, L. Berthier, and F. Zamponi, Nature of excitations and defects in structural glasses, Nat. Commun. **10**, 5102 (2019).

[51] J. T. Parley, R. Mandal, and P. Sollich, Mean-field description of aging linear response in athermal amorphous solids, Phys. Rev. Materi. **6**, 065601 (2022).

[52] H. J. Hwang, R. A. Riggleman, and J. C. Crocker, Understanding soft glassy materials using an energy landscape approach, Nat. Mater. **15**, 1031 (2016).

[53] P. K. Morse and E. I. Corwin, Geometric signatures of jamming in the mechanical vacuum, Phys. Rev. Lett. **112**, 115701 (2014).

[54] P. K. Morse and E. I. Corwin, Echoes of the glass transition in a thermal soft spheres, Phys. Rev. Lett. **119**, 118003 (2017).

[55] W. Kob and J.-L. Barrat, Aging effects in a Lennard-Jones glass, Phys. Rev. Lett. **78**, 4581 (1997).

[56] P. Mendoza-Méndez, R. Peredo-Ortiz, E. Läzaro-Lázaro, M. Chávez-Paez, H. Ruiz-Estrada, F. Pacheco-Vázquez, M. Medina-Noyola, and L. F. Elizondo-Aguilera, Structural relaxation, dynamical arrest, and aging in soft-sphere liquids, J. Chem. Phys. **157**, 244504 (2022).

[57] L. E. Silbert, A. J. Liu, and S. R. Nagel, Vibrations and diverging length scales near the unjamming transition, Phys. Rev. Lett. **95**, 098301 (2005).

[58] A. Ikeda, L. Berthier, and G. Biroli, Dynamic criticality at the jamming transition, J. Chem. Phys. **138**, 12A507 (2013).

[59] A closely related effect was reported in Ref. [60], which showed that the "boson peak" frequency $\omega_{\rm bp}$ defined by the maximum of $D(\omega)/\omega$ in small-molecule glasses [61] increased with increasing annealing time.

[60] N. V. Surovtsev, A. P. Shebanin, and M. A. Ramos, Density of states and light-vibration coupling coefficient in B_2O_3 glasses with different thermal history, Phys. Rev. B **67**, 024203 (2003).

[61] A. P. Sokolov, A. Kisliuk, M. Soltwisch, and D. Quitmann, Medium-range order in glasses: Comparison of Raman and diffraction measurements, Phys. Rev. Lett. **69**, 1540 (1992).